Equatorial Long Waves in Geostationary Satellite Observations and in a Multichannel Sea Surface Temperature Analysis

Richard Legeckis,[1] William Pichel,[1] and George Nesterczuk[2]

Abstract

Geostationary satellite observations of a zonally oriented sea surface temperature front in the eastern equatorial Pacific were made between 1975 and 1981. Long waves appeared along the front mainly during the summer and fall, except during 1976, the year of an El Niño. The waves have averaged periods of 25 days and wavelengths of 1000 km. At the end of 1981, the long waves also were detected in a new sea surface temperature analysis based on multichannel infrared measurements from a polar-orbiting satellite. This quantitative analysis may improve the ability to resolve low-frequency equatorial wave motions from satellite observations.

1. Introduction

Equatorial ocean currents are known to be unstable. In a linear stability analysis, Philander (1978) showed that the horizontal shear zone between the south equatorial current and the north equatorial countercurrent allows the growth of long waves that have a wavelength of 1000 km and a period of about 25 days. Semtner and Holland (1980) used a 3-dimensional baroclinic wind-driven numerical model to demonstrate the instability of equatorial currents. Cox (1980) showed that meridional asymmetries in the wind field produce a corresponding asymmetry in the long-wave response. Moore and Philander (1977) presented a summary of the modeling of tropical ocean circulation.

Direct measurements of equatorial long waves are relatively recent. Düing *et al.* (1975) observed westward-propagating long waves in the Atlantic equatorial undercurrent. Harvey and Patzert (1976) reported long-wave oscillations at a depth of 3300 m in current meter records taken west of the Galápagos Islands in the Pacific. Hayes (1979) found oscillations of 40–60 days near the bottom at three sites north of the equator in the eastern and central Pacific. Wyrtki (1978) used sea level measurements at Fanning Island in the Pacific to describe long waves with a period of 34 days. Weisberg *et al.* (1979) used current meter and hydrographic observations in the Gulf of Guinea to identify equatorially trapped Rossby-gravity waves.

Equatorial long waves also have been observed in geostationary satellite remotely sensed infrared images. Legeckis (1977) showed that a zonally oriented sea surface temperature (SST) front north of the equator in the eastern equatorial Pacific took on a wavelike shape. Successive positions of the wave crests have been used to estimate a nominal wavelength of 1000 km and westward directed phase speed of 40 km/day. Equatorial long waves were monitored by the geostationary satellite between 1975 and 1981, and the space-time variations of these waves are presented in this study. However, there are several limitations in the use of the geostationary satellite infrared images for tracking equatorial long waves. The method used to identify the position of the equatorial SST front is both subjective and qualitative. Furthermore, the SST front has been detected only seasonally between May and December. This is due to a combination of the seasonal decrease of equatorial SST gradients along with the limitations of the GOES satellite in resolving the SST gradients in the presence of a relatively moist tropical atmosphere.

Recent improvements in the automated global sea surface temperature analysis at the National Earth Satellite Service (NESS) appear to offer a quantitative tool for tracking equatorial long waves. It will be shown that the use of polar-orbiting satellite infrared measurements at several different wavelengths (3.7, 11, 12 μm) allows SST maps that are capable of resolving the signature of equatorial long waves to be constructed. A two-month automated SST analysis of the equatorial Pacific is presented to illustrate these improvements.

2. Equatorial long waves in geostationary satellite observations

There exists a zonally oriented SST front in the eastern equatorial Pacific that is usually found to the north of the equator and west of South America, as illustrated in Fig. 1. West of the Galápagos Islands, this front is often wavelike, with sharp peaks and wide troughs. Based on satellite infrared images obtained in 1975, Legeckis (1977) estimated that the waves observed along the SST front move westward at an av-

[1] National Earth Satellite Service, Washington, D.C. 20233.
[2] EG&G Analytical Services, Inc., Riverdale, Md. 20840.

© 1983 American Meteorological Society

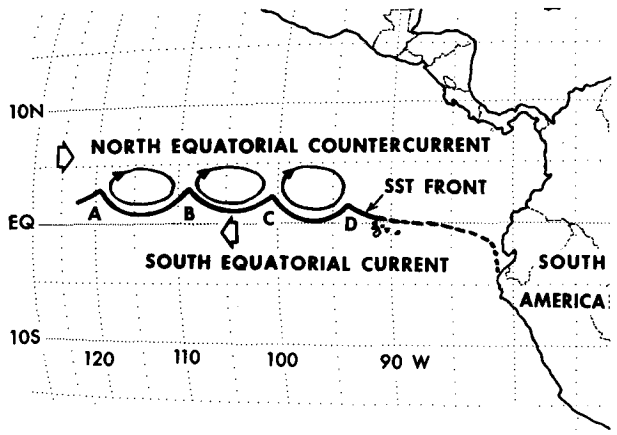

FIG. 1. The schematic representation of the wave-like sea surface temperature front in the eastern equatorial Pacific. The letters refer to distinct wave peaks observed in the satellite infrared images. The anticyclonic, eddy-like circulation patterns are inferred from drifting buoy tracks.

erage speed of 40 km/day with a wavelength of about 1000 km.

In the summer of 1979, several drifting buoys were used to establish the circulation patterns north of the equatorial SST front. Hansen *et al.* (1980) described large-scale, anticyclonic, eddy-like motions that translate westward at the same speed as the long waves along the front. The eddy centers were found to coincide with the broad wave troughs observed in satellite infrared imagery, as illustrated in Fig. 1. However, due to the persistent cloud cover at the intertropical convergence zone (ITCZ), the eddies never have been observed in the satellite images, and our only clue to their existence comes from the combined measurements of the drifting buoys and the position of the long waves along the SST front.

The initial satellite observations of the long waves reported by Legeckis (1977) were based on GOES infrared images enhanced for the SST range in the equatorial Pacific during October and November 1975. Subsequently, an attempt was made to determine if the waves also were present earlier in 1975. Since enhanced GOES images were not available earlier than October, digital data were reprocessed selectively at NASA's Goddard Space Flight Facility (GSFC) to locate the equatorial SST front. Nesterczuk *et al.* (1980) reported that long waves were present in the equatorial Pacific between May and November of 1975. However, due to the cost of reprocessing the GOES data, sufficient samples of processed data were not available to resolve the wave motion without aliasing. To provide more continuity of satellite observations of long waves, a project was started at NESS to produce near real-time enhanced GOES images of the equatorial Pacific. This project was sponsored by NOAA's Equatorial Pacific Ocean Climate Study (EPOCS). However, the position of the equatorial SST front could not be established in the GOES images during 1976. It generally is accepted that an El Niño occurred during 1976 and it is probable that the associated warming of the equatorial waters limited the magnitude of the SST gradients, making the waves undetectable in the geostationary images.

Between 1977 and 1981, the equatorial long waves appeared seasonally each year in the GOES infrared images, as described by Legeckis (1982). Typically, the mean position of the equatorial SST front was established by comparing 6 to 12 infrared images each day. On this time scale, the SST front remained nearly stationary and could be distinguished from clouds moving at shorter time scales. The space-time variability of long waves in the eastern equatorial Pacific from 1975 to 1981 is summarized in Fig. 2. Each phase line (identified by letter A, B, C . . .) represents a locus of a wave crest projected on the equator. The separation between adjacent phase lines along the equator on a given day provides an estimate of the wavelength, while the separation along a fixed longitude provides an estimate of the wave period. The satellite observations during 1975 were not complete, and the dashed phase lines in Fig. 2 are the best guess based on several available data points, as described by Nesterczuk *et al.* (1980). Between 1977 and 1981, the wavelengths had a range of from 400 to 1450 km, with a mean of nearly 1000 km, and the wave period had a range of from 13 to 35 days, with a mean of nearly 25 days.

There appears to be significant differences in the onset, duration, and period of the waves each year. For example, during 1977 and 1980 the waves were not observed until July, while in the other years the waves first were observed during May. After onset, the waves are most active for about four to six months. During this time, they extend far westward and exhibit large amplitudes (200–400 km north–south). The most extreme westward extent of the equatorial waves observed to date appears to have occurred in 1975. Wyrtki (1978) suggested that the 34-day oscillations in the sea level record at Fanning Island (4°N, 159°W) in 1975 were the result of westward-moving long waves originating in the eastern Pacific. There is considerable variability in the wave periods. From 1977 to 1979, several of the phase lines in Fig. 2 appear to have a time scale of 30 days, similar to the mean period predicted by Cox (1980) in a numerical model of long waves. Time scales shorter than 30 days are evident during most of 1981. Towards the end of a seasonal cycle, the waves with the shorter length and time scales tend to be found between 90°W and 100°W. Occasionally transient events with shorter time scales appear farther to the west, as in the case of phase line B during 1980. It also is possible that long gaps (~7 days) in our satellite observations due to persistent cloudiness occasionally prevent the resolution of the shorter time-scale events.

3. Multichannel analysis

Until 1981, a computer processing system called GOSSTCOMP was used at NESS to produce the global sea surface temperature maps, as described by Brower *et al.* (1976). Cloud discrimination and atmospheric moisture corrections were provided by a vertical temperature profiling radiometer (VTPR). These atmospheric measurements were combined with single-channel infrared observations from a scanning radiometer (SR) to estimate the SST. Barnett *et al.* (1979) showed that the ocean temperatures provided by GOSSTCOMP were biased by 1–4°C with respect to *in situ* observa-

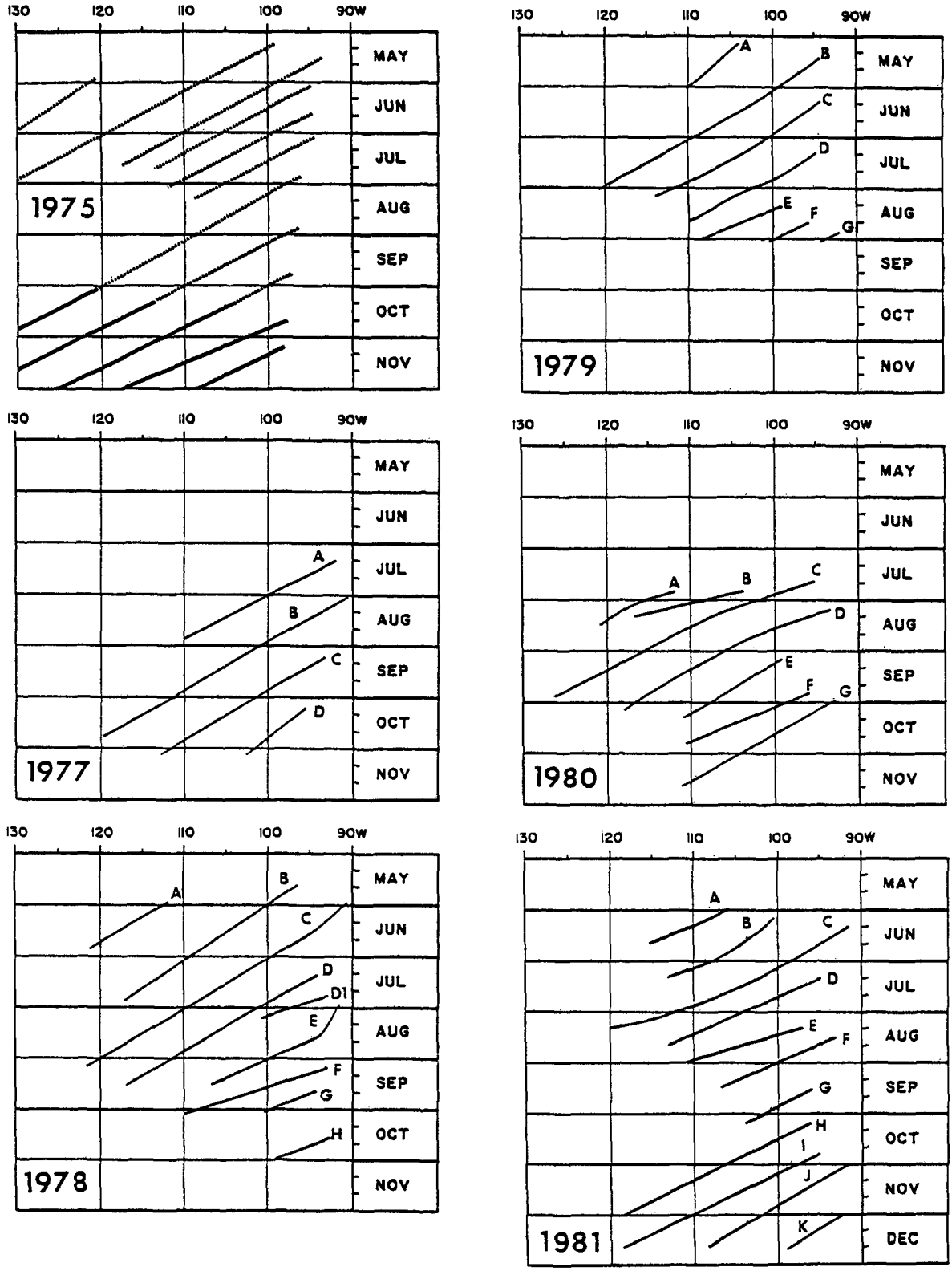

FIG. 2. Each phase line (A through K) of the equatorial long waves is the locus of a wave crest projected on the equator with time during each year from 1975 to 1981. The wave crests were identified in geostationary satellite (GOES) infrared images at a zonally oriented sea surface temperature front. The waves were not observed during 1976. The dashed lines during 1975 indicate that the phase was estimated from only a few samples and may be aliased.

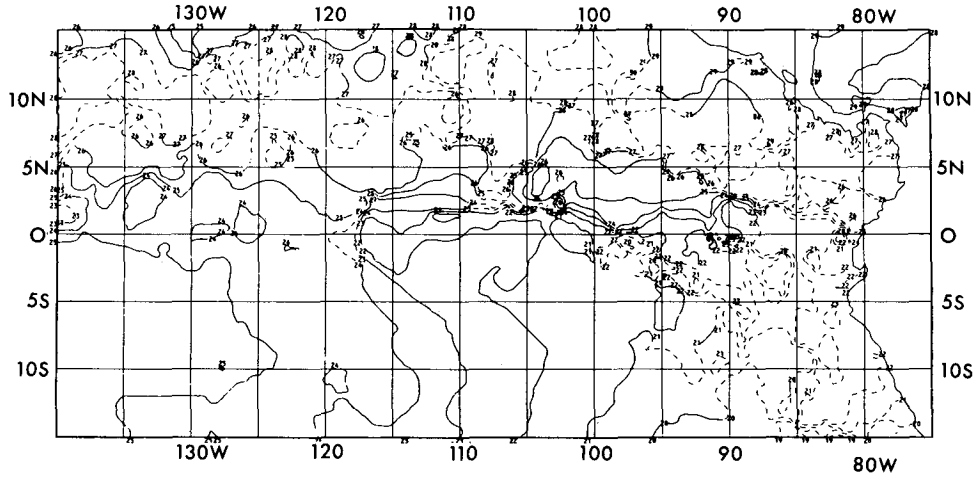

FIG. 3. The mean sea surface temperature contours at 1°C increments for the seven days ending on 6 October 1981, from the GOSSTCOMP analysis in the eastern equatorial Pacific. Dashed contours indicate that satellite observations are older than seven days.

tions.

Late in 1981, a new technique was introduced at NESS to make use of multichannel infrared measurements available from the Advanced Very High Resolution Radiometer (AVHRR) on the TIROS polar-orbiting satellites (Schwalb, 1978). The new multichannel procedures for estimating sea surface temperatures (MCSST) are described by Pichel (1981). The differences in energy emitted from the sea surface at several wavelengths (3.7, 11, 12 μm) are used to estimate the corrections for atmospheric attenuation and to discriminate cloud-free ocean areas. Individual SST observations are made at a spatial scale of 8 km, with a separation of 25 km between each observation. An objective analysis technique is used to prepare temperature contour charts at several scales. A global SST analysis is produced daily at a spatial resolution of 100 km. The coastal waters of the United States and the equatorial Pacific are analyzed weekly at a resolution of 50 km. These maps are archived on microfilm by the Environmental Data and Information Service (EDIS).

McClain *et al.* (1982) described the algorithm used in the MCSST analysis to estimate the atmospheric moisture corrections from multichannel differences. The atmospheric transmittance models described by Weinreb and Hill (1980) were applied to a set of cloud-free radiosondes. The theoretically predicted temperatures were then compared to a set of colocated, fixed-buoy SST measurements. It was found that predicted temperatures were lower than *in situ* observations and a temperature-dependent bias correction was added to the theoretically predicted SST. McClain *et al.* (1982) reported that satellite-derived SST measurements based on the bias-corrected multichannel measurements used in the MCSST analysis agreed with fixed-buoy measurements near the surface, with a near-zero bias and within an rms error of 0.7°C. Bernstein (1982) made an independent study of multichannel

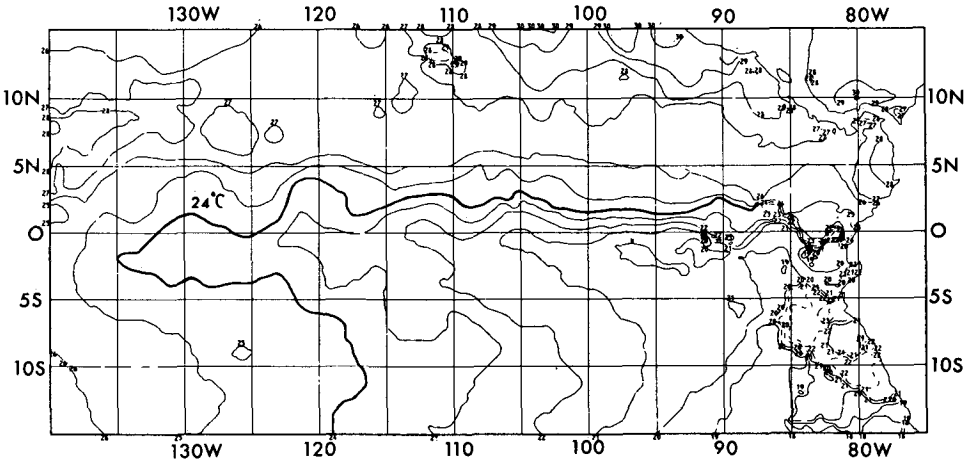

FIG. 4. The mean sea surface temperature contours at 1°C increments for the seven days ending on 13 October 1981, from the MCSST analysis in the eastern equatorial Pacific. Dashed contours indicate that satellite observations are older than seven days. The 24°C contour indicates the approximate location of the equatorial SST front.

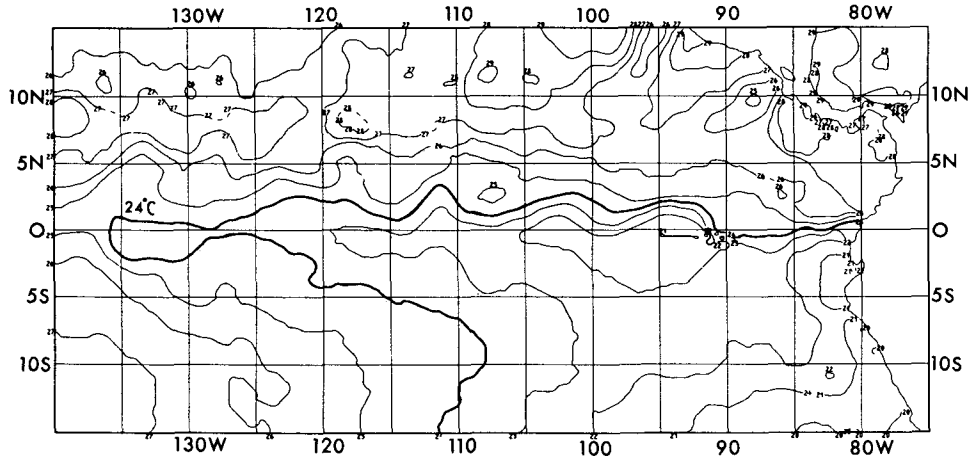

FIG. 5. The mean sea surface temperature contours at 1°C increments for the seven days ending on 8 December 1981, from the MCSST analysis in the eastern equatorial Pacific. The 24°C contour indicates the approximate location of the equatorial SST front.

AVHRR and ship buoy measurements for a wide range of tropical and subtropical conditions and found that the satellite measurements were accurate to within 0.6°C. This is a considerable improvement over the SST estimated by GOSSTCOMP using the single channel SR measurements.

4. Equatorial long waves in the multichannel SST analysis

An initial attempt was made to locate the equatorial waves in the daily global SST maps derived from multichannel observations and available on microfilm at a spatial resolution of 100 km. Although some wave peaks could be identified, there appeared to be a lack of continuity in successive observations. It was postulated that by using the 50 km spatial scale available in the multichannel observations, the spatial resolution of the sharp wave crests evident in Fig. 1 would be improved. Furthermore, to allow a sufficient number of cloud-free satellite observations to update the analysis, seven days of observations were composited for each SST map using an objective analysis scheme. The subsequent comparison of the weekly 50 km SST fields allowed the equatorial waves to be tracked along the zonally oriented SST front north of the equator.

The transition to the use of the multichannel observations was made on 7 October 1981. The seven-day objective analysis for the week ending 6 October is shown in Fig. 3. The seven-day MCSST analysis for the week ending 13 October is shown in Fig. 4. Both SST maps are prepared at a spatial resolution of 50 km in the eastern equatorial Pacific. The most apparent change between Fig. 3 and Fig. 4 is the smoother

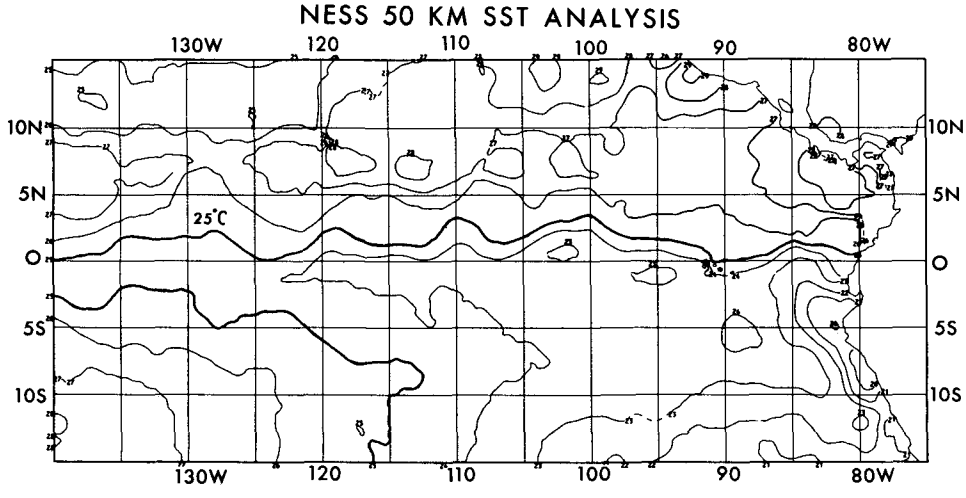

FIG. 6. The mean sea surface temperature contours at 1°C increments for the seven days ending on 29 December 1981, from the MCSST analysis in the eastern equatorial Pacific. The 25°C contour indicates the approximate location of the equatorial SST front.

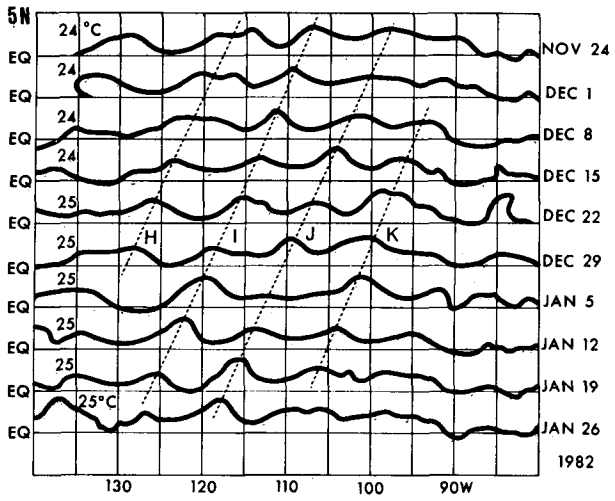

FIG. 7. Each sea surface temperature contour (24°C or 25°C) represents the approximate position of a zonally oriented sea surface temperature front north of the equator in the eastern Pacific. The contours were selected from seven-day MCSST analyses as shown in Fig. 5 and Fig. 6. The phase lines H through K indicate the apparent westward propagation of long waves along the front. These phase lines also appeared during December 1981 in the geostationary satellite observations illustrated in Fig. 2.

SST contour field in the MCSST analysis in Fig. 4. This is attributed to the larger number and improved resolution of satellite observations in the MCSST analysis. For example, the dashed contours in Fig. 3 and Fig. 4 indicate that the satellite measurements are older than seven days. The lack of recent satellite observations near the coast of South America in Fig. 4 is attributed to the fact that the initial MCSST analysis used only the nighttime (0300 local equatorial crossing) AVHRR data from the NOAA-7 satellite. This analysis was improved in subsequent weeks by including daytime (1500 local equatorial crossing) data.

A second change evident in comparing Fig. 3 and Fig. 4 is the improved distribution of the zonal and meridional SST gradients in the vicinity of the equator in Fig. 4. The MCSST analysis in Fig. 4 bears a striking resemblance to the SST field predicted by Cox (1980) in a numerical model of equatorial circulation. For example, the cooler water associated with the South Equatorial Current appears at the equator in Fig. 4. This is accompanied by an eastward decrease of temperatures along the equator between 140°W and 90°W. The zonally oriented SST front north of the equator in Fig. 4 is distorted by a series of wave-like features that resemble the equatorial long waves described by Cox (1980). South of the equator, the SST contour field is zonally oriented near 10°S. These SST features persist with time, as illustrated in the MCSST analysis for the week of 8 December in Fig. 5 and for the week of 29 December in Fig. 6.

To illustrate the low-frequency wave motion at the zonally oriented SST front in the MCSST analysis, a space-time diagram of selected temperature contours between 24 November 1981 and 26 January 1982 is shown in Fig. 7. The 24°C and 25°C contours were selected because they appear to be most representative of the long waves in the weekly SST maps as shown in Figs. 5 and 6. The dashed phase lines (H, I, J, K) in Fig. 7 suggest the westward displacement of individual wave crests along the SST front. The phase lines in Fig. 7 appear in nearly the same position as those measured in the analysis of wave crest displacements from the GOES observations during 1981, as shown in Fig. 2. The separation between phase lines (wavelength) is on the order of 1000 km and the wave period is 30 days. The comparison between the MCSST and the GOES-derived phase lines could not be extended beyond December 1981, since the equatorial SST front became too obscure in the GOES infrared imagery. The persistence of the wave crests in the MCSST analysis during January 1982 suggests that the quantitative analysis will provide a superior method for the detection and tracking of equatorial waves. A complete year of observations will have to be made to allow a final assessment of the GOES and the MCSST analysis methods, but these initial results are very encouraging.

5. Conclusions

The geostationary satellite infrared observations of the equatorial Pacific have proved to be useful in identifying and tracking equatorial long waves. The space-time representation of the long waves in Fig. 2 summarizes the seasonal events from 1975 to 1981. The equatorial waves were not observed in the geostationary satellite images during the summer of 1976. Since this occurred during the El Niño of 1976, the geostationary satellite observation of the equatorial SST front may provide a qualitative index of future El Niño events. The new multichannel sea surface temperature algorithms introduced at NESS late in 1981 offer a quantitative method for monitoring equatorial waves. These analyses should be useful since they form a direct link to the SST output of ocean numerical circulation models.

It has been suggested by Philander (1978) that the long waves derive their energy from the shear between the westward-flowing South Equatorial Current and the eastward-flowing North Equatorial Countercurrent. Cox (1980) showed that the peak wave activity closely follows the peak shear of the mean currents in a wind-driven ocean circulation model. Using a 20-year monthly average wind field taken between the early 1950s and early 1970s as described by Wyrtki and Meyers (1976), Cox (1980) showed that the peak wave response occurs in late summer. The satellite observations summarized in Fig. 2 suggest that there is considerable annual and interannual variability in the wave response. These differences between the numerical model and satellite observations could be resolved in the future provided the concurrent wind fields are used.

Acknowledgments. The study was supported by the National Oceanic and Atmospheric Administration's EPOCS project: EPOCS Contribution No. 017. The study by Nesterczuk was supported by NASA contract NAS-5-24467 at GSFC. We thank Philip Hovey, Karen Czuba, and Simon Roman for the illustrations and Madelyn Bowman for preparation of the manuscript.

References

Barnett, T. P., W. C. Patzert, S. C. Webb, and B. R. Bean, 1979: Climatological usefulness of satellite determined sea surface temperatures in the tropical Pacific. *Bull. Am. Meteorol. Soc.*, **60**, 197–205.

Bernstein, R. L., 1982: Sea surface temperature estimation using the NOAA-6 satellite Advanced Very High Resolution Radiometer. *J. Geophys. Res.*, **87**, 9455–9465.

Brower, R. L., H. S. Gohrband, W. G. Pichel, T. L. Signore, and C. C. Walton, 1976: Satellite derived sea surface temperatures from NOAA spacecraft. *NOAA Tech. Memo. NESS 78*, Washington, D.C., pp. 1–74.

Cox, M. D., 1980: Generation and propagation of 30-day waves in a numerical model of the Pacific. *J. Phys. Oceanogr.*, **10**, 1168–1186.

Düing, W., P. Hisard, E. Katz, J. Knauss, J. Meincke, L. Miller, K. Moroshkin, G. Philander, A. Rybnikov, K. Voigt, and R. Weisberg, 1975: Meanders and long waves in the equatorial Atlantic. *Nature*, **257**, 280–284.

Hansen, D. V., C. A. Paul, and R. Legeckis, 1980: Comparison of satellite and direct current observations of long waves in the eastern tropical Pacific during FGGE. *Trans. Am. Geophys. Union*, **61**.

Harvey, R. R., and W. C. Patzert, 1976: Deep current measurements suggest long waves in the eastern equatorial Pacific. *Science*, **193**, 883–885.

Hayes, S. P., 1979: Benthic current observations at DOMES sites A, B and C in the tropical North Pacific Ocean. In *Marine Geology and Oceanography of the Pacific Manganese Nodule Province*, edited by J. L. Bischoff and D. Z. Piper, Plenum Press, New York, N.Y., pp. 83–112.

Legeckis, R., 1977: Long waves in the eastern equatorial Pacific Ocean: A view from a geostationary satellite. *Science*, **197**, 1179–1181.

——, 1982: Geostationary satellite observations of long waves in the eastern equatorial Pacific—1975–1981. *NOAA Tech. Rept. NESS 92*, pp. 1–22.

McClain, E. P., W. Pichel, C. Walton, Z. Ahmed, and J. Sutton, 1982: Multichannel improvements to satellite derived global sea surface temperatures, *Preprints, XXIV COSPAR (Ottawa)*, NOAA/NESS, Washington, D.C.

Moore, D., and S. G. H. Philander, 1977: Modeling of the tropical ocean circulation. In *The Sea*, Vol. 6, Wiley Interscience, New York, N.Y., pp. 316–361.

Nesterczuk, G., R. Legeckis, and P. Schmid, 1980: Satellite observations of the eastern Pacific equatorial front—1975. *Rept. 001-80*, EG&G Analytical Services, Inc., Riverdale, Md., pp. 1–48.

Philander, S. G. H., 1978: Instabilities of zonal equatorial currents: II. *J. Geophys. Res.*, **83**, 3679–3682.

Pichel, W. G. 1981: Multichannel critical design. *NESS Int. Doc.*, Washington, D.C., pp. 1–45.

Schwalb, A., 1978: The TIROS-N/NOAA A-G satellite series. *NOAA Tech. Memo. NESS 95*, Washington, D.C., pp. 1–75.

Semtner, A. J., and W. R. Holland, 1980: Numerical simulation of equatorial ocean circulation, Part I: A basic case in turbulent equilibrium. *J. Phys. Oceanogr.*, **10**, 667–693.

Weinreb, M. P., and M. L. Hill, 1980: Calculations of atmospheric radiance and brightness temperatures in infrared window channels of satellite radiometers. *NOAA Tech. Rept. NESS 80*, Washington, D.C., pp. 1–40.

Weisberg, R. H., A. Horigan, and C. Colin, 1979: Equatorially trapped Rossby-gravity wave propagation in the Gulf of Guinea. *J. Mar. Res.*, **37**, 67–86.

Wyrtki, K., 1978: Lateral oscillations of the Pacific Equatorial Countercurrent. *J. Phys. Oceanogr.*, **8**, 530–532.

——, and G. Meyers, 1976: The trade wind field over the Pacific Ocean. *J. Appl. Meteorol.*, **15**, 698–704.

announcements (*continued from page 132*)

Stratospheric balloon intercomparison campaign

Four huge balloons, carrying several tons of scientific apparatus to measure simultaneously the vertical profiles of key chemical constituents in the stratosphere, were launched on 22 September 1982 from the National Scientific Balloon Facility (NSBF) in Palestine, Tex., making the first phase of a seven nation Balloon Intercomparison Campaign (BIC) successful. Within three and one-half hours, 13 remote-sensing instruments, using eight different techniques, and one in-situ instrument were launched.

The balloon payloads ranged from 680 kg, requiring a 765 000 m^3 balloon, up to nearly 1800 kg, using a 1 190 000 m^3 balloon. Three of the four gondolas achieved the goal of the mission, which was to fly for approximately 24 h at latitudes between 38.5 and 41 km, but one gondola had to be parachuted down after 20 min due to a defective balloon. The instruments were recovered and this gondola was successfully reflown on 5 October 1982.

The balloon-borne instruments measuring vertical profiles were complemented by both ground-based instruments, located at Holloman Air Force Base in New Mexico and at Kitt Peak National Observatory in Arizona, and an aircraft-borne spectrometer which has flown on the National Center for Atmospheric Research (NCAR) Sabreliner to measure the column content of several of the same atmospheric constituents. Another important aspect of the BIC has been to determine as much as possible about the meteorological properties of the air mass in which the measurements are made. Scientists from the Atmospheric Environment Service (AES-Canada) launched small radiosonde balloons every 6 h before and during the mission. In addition, satellite data from the TIROS series were used to provide analysis of air mass trajectories on a hemispheric scale. This initial phase of BIC marks the first time that such a complete set of measurements on key chemical constituents has been carried out simultaneously on a single, well-defined air mass.

A meeting of BIC participants has been scheduled for July 1983 to discuss the results of the Fall Phase I Campaign, and a series of publications is planned. For further information on BIC, contact either Robert T. Watson, EBT-8, NASA Headquarters, Washington, D.C. 20546 or Phil Gamlen, ICI Americas Inc., Wilmington, Del. 19897.

(*continued on page 147*)